Unified Performance Analysis of C–MRC and LAR Decode–and–Forward Schemes

Amir Nasri[†], Robert Schober[†], and Murat Uysal[††]

[†]University of British Columbia, Canada, [††]University of Waterloo, Canada

Abstract

In this paper, we study the performance of two important types of decode–and–forward (DF) relaying schemes proposed for cooperative diversity (CD) systems, namely, cooperative maximum–ratio combining (C–MRC) and link adaptive regeneration (LAR). In particular, we provide a unified framework for the error rate performance analysis of C–MRC, LAR–α_{inst}, and LAR–α DF schemes for multi–branch CD systems consisting of a source, a destination, and multiple relays. Based on this framework, we provide accurate expressions for the performance of the considered CD systems for high signal–to–noise ratios and Rayleigh fading. The developed asymptotic performance results facilitate a performance comparison with other relaying schemes and reveal that while full diversity is achieved by C–MRC and LAR–α_{inst}, LAR–α is, in general, unable to collect full diversity.

I. INTRODUCTION

Cooperative diversity (CD) is a promising technique that enables high spatial diversity gains in distributed wireless networks by allowing idle wireless nodes to relay signals emitted by a source node to a destination node. This signal relaying can be performed according to two important class of relaying techniques, namely, decode–and–forward (DF) and amplify–and–forward (AF). Compared to AF relaying, DF relaying eliminates the need for analog signal storage and expensive RF chains [1, 2], and as a result, is considered to have a greater potential to be employed in future wireless standards.

The combining scheme used at the destination plays an essential role in the performance of DF cooperative diversity systems. It is well–known that conventional maximum ratio combining (MRC) does not offer full diversity in the presence of detection errors at the relays [3]. To overcome this problem, various combining schemes have been proposed in the literature. In particular, a maximum–likelihood (ML) combiner was proposed in [3] assuming binary signaling. However, the complexity of the ML metric becomes prohibitive specially for high order signal constellations. A piece–wise linear approximation for the ML metric was advocated in [4] which leads to a tractable performance

analysis, but is, in general, unable to collect full diversity. To avoid the problems associated with the ML combining, λ–MRC has been proposed in [3]. While this combining scheme provides a similar performance as ML combining, it suffers from high computational complexity as the optimal value for the combining weight λ may not be obtained in closed form. To overcome this problem, cooperative MRC (C–MRC), a variant of λ–MRC, was proposed in [1] which achieves a performance close to that of ML combining but at a much lower complexity, regardless of the size of the employed signal constellation. Furthermore, two related DF schemes based on the link adaptive regeneration (LAR) concept, namely LAR–α_{inst} and LAR–α, were proposed in [5]. In LAR, variable gains are used at the relays to adaptively adjusting the instantaneous transmit power to variations in the source–relay and relay–destination links. Due to their low implementation complexity and desirable error rate performance, C–MRC and LAR constitute two types of most practically relevant DF schemes, and therefore, a unified study of their performance is of both theoretical and practical interest.

The diversity gain of C–MRC was analyzed in [1] while the diversity gain achieved by LAR–α_{inst} and LAR–α was studied in [5]. Furthermore, the asymptotic performance of C–MRC has been analyzed in [6] for the case of a single–relay CD system. However, an accurate performance analysis of C–MRC, LAR–α_{inst}, and LAR–α in a more practical scenario involving multiple relays is not available in the literature. Motivated by this, in this letter, we provide a unified framework for the performance analysis of multi–branch CD systems consisting of a source, a destination, and multiple relays, where relaying is performed according to C–MRC, LAR–α_{inst}, or LAR–α. Based on this framework, we develop accurate expressions for the performance of the considered CD system for high signal–to–noise ratios (SNRs) and Rayleigh fading. The developed asymptotic performance results are valid for arbitrary modulation formats and arbitrary channel qualities and facilitate a performance comparison with other relaying schemes. Furthermore, these results reveal that C–MRC and LAR–α_{inst} achieve the maximum possible diversity gain equal to the number of paths between the source and the destination, whereas LAR–α is, in general, unable to collect full diversity.

The remainder of this letter is organized as follows. In Section II, the system model for the considered CD system is introduced. In Section III, asymptotic expressions for the symbol error rate (SER) and bit error rate (BER) as well as the diversity gain are obtained for C–MRC, LAR–α_{inst}, and LAR–α. Numerical and simulation results are presented in Section IV, and conclusions are drawn in Section V.

Notation: In this paper, $[\cdot]^T$, $(\cdot)^*$, $\Re\{\cdot\}$, and $\mathcal{E}_x\{\cdot\}$ denote transposition, complex conjugation, the

real part of a complex number, and statistical expectation with respect to x, respectively. Furthermore, we use the notation $u \doteq v$ to indicate that u and v are asymptotically equivalent, and a function $f(x)$ is $o(g(x))$ if $\lim_{x \to 0} f(x)/g(x) = 0$.

II. SYSTEM MODEL

The considered CD system consists of a source S, a destination D, and K cooperating relays R_k, $1 \le k \le K$, and employs C–MRC [1], LAR–α_{inst}, or LAR–α [5] for relaying (Fig. 2). Transmission from the source to the destination is organized in two hops. In the first hop, the source transmits and the relays and the destination receive. The signals received at the relays and the destination in the first hop are given by

$$r_{1k} = \sqrt{p_s}\, h_{1k} x + n_k, \qquad 1 \le k \le K \tag{1}$$

$$r_0 = \sqrt{p_s}\, h_0 x + n_0, \tag{2}$$

respectively, where p_s is the average transmit symbol power of the source and x denotes the symbol transmitted by the source. We assume $x \in \mathcal{X}$, where $\mathcal{X}$ is an M–ary constellation such as binary phase–shift keying (BPSK) or M–ary phase–shift keying (M–PSK). Furthermore, we assume x is normalized such that $\mathcal{E}\{|x|^2\} = 1$. In (1) and (2), h_0 and h_{1k} are the fading gains of the source–destination channel and the channel between the source and the relay R_k, respectively. Furthermore, n_0 and n_{1k} denote the Gaussian distributed noise samples at, respectively, the destination in the first hop and the kth relay in the first hop. The variances of these noise samples are denoted by $\sigma_{n_0}^2 \triangleq \mathcal{E}\{|n_0|^2\}$ and $\sigma_{n_{1k}}^2 \triangleq \mathcal{E}\{|n_{1k}|^2\}$, respectively. After receiving the signal r_{1k}, relay R_k, $1 \le k \le K$, performs coherent ML detection to obtain the decoded symbol $\hat{x}_k$ as

$$\hat{x}_k = \arg\min_{x \in \mathcal{X}} |r_{1k} - \sqrt{p_s}\, h_{1k} x|^2. \tag{3}$$

In the second hop, relay R_k, $1 \le k \le K$, multiplies the decoded symbol $\hat{x}_k$ with factor $\sqrt{p_s \alpha_k}$ and forwards the resulting signal to the destination. Here, $\alpha_k \in [0, 1]$, $1 \le k \le K$, is the relay gain which depends on the adopted DF scheme and will be discussed later in this section. The signal received from the kth relay at the destination in the second hop, r_{2k}, can therefore be modeled as

$$r_{2k} = \sqrt{p_s \alpha_k}\, h_{2k}\, \hat{x}_k + n_{2k}, \qquad 1 \le k \le K, \tag{4}$$

where h_{2k} denotes the gain of the channel between relay R_k and the destination and n_{2k} is the Gaussian distributed noise at the destination in the second hop with variance $\sigma_{n_{2k}}^2 \triangleq \mathcal{E}\{|n_{2k}|^2\}$.

We assume independent Rayleigh fading for all transmitter–receiver pairs [1, 2, 5, 7]. Thus, the fading gains $h_0 \triangleq a_0 \, \mathrm{e}^{-j\theta_0}$, $h_{1k} \triangleq a_1 \, \mathrm{e}^{-j\theta_1}$, and $h_{2k} \triangleq a_2 \, \mathrm{e}^{-j\theta_2}$, are independent Gaussian random variables (RVs) with zero mean and variances $\Omega_0 \triangleq \mathcal{E}\{|h_0|^2\}$, $\Omega_{1k} \triangleq \mathcal{E}\{|h_{1k}|^2\}$, and $\Omega_{2k} \triangleq \mathcal{E}\{|h_{2k}|^2\}$, respectively. The channel amplitudes a_0, a_{1k}, and a_{2k} are positive real RVs and follow a Rayleigh distribution. Furthermore, the channel phases θ_0, θ_{1k}, and θ_{2k} are uniformly distributed in $[-\pi, \pi)$ and are independent from the channel amplitudes. For future reference, we define the instantaneous SNRs associated with the source–destination link, the source–relay links, and the relay–destination links as $\gamma_0 \triangleq p_s \, a_0^2/\sigma_{n_0}^2$, $\gamma_{1k} \triangleq p_s \, a_{1k}^2/\sigma_{n_{1k}}^2$, and $\gamma_{2k} \triangleq p_s \, a_{2k}^2/\sigma_{n_{2k}}^2$, respectively. The corresponding average SNRs are given by $\bar{\gamma}_0 = p_s \, \Omega_0/\sigma_{n_0}^2$, $\bar{\gamma}_{1k} = p_s \, \Omega_{1k}/\sigma_{n_{1k}}^2$, and $\bar{\gamma}_{2k} = p_s \, \Omega_{2k}/\sigma_{n_{2k}}^2$.

Having received the signals r_0 and r_{2k} from the source and the relay, respectively, the destination performs diversity combining to obtain the estimate $\hat{x} = \arg\min_{\tilde{x} \in \mathcal{X}} m_c(\tilde{x})$. The decision metric $m_c(\tilde{x})$ is defined as

$$m_c(\tilde{x}) \triangleq \frac{|r_0 - \sqrt{p_s}h_0\tilde{x}|^2}{\sigma_{n_0}^2} + \lambda_k \frac{|r_{2k} - \sqrt{p_s\alpha_k}\,h_{2k}\tilde{x}|^2}{\sigma_{n_{2k}}^2}, \tag{5}$$

where $\tilde{x} \in \mathcal{A}$ is a trial symbol. Furthermore, the combining weight $\lambda_k \in [0, 1]$, $1 \leq k \leq K$, depends on the adopted DF scheme and will be discussed shortly.

Relay Gain α_k***:*** This factor is defined in Table I for C–MRC, LAR–α_{inst}, and LAR–α. For C–MRC $\alpha_k = 1$ is valid and therefore no scaling is performed at the relay. For LAR–α_{inst} and LAR–α, however, a variable gain α_k is used to appropriately adjust the instantaneous power at the kth relay to variations in the respective source–relay and relay–destination links.

Combining Weight λ_k***:*** This factor is also defined in Table I for the considered DF schemes. For C–MRC, a variable weight $\lambda_k < 1$ is assigned to the signal received from the relay in order to take into account the effect of possible erroneous decisions at the kth relay. For LAR–α_{inst} and LAR–α $\lambda_k = 1$ is valid, i.e., the destination performs conventional MRC as due to proper power scaling at the relay additional processing is not required at the destination.

Signaling Requirements: Since the three considered DF schemes employ different relay gains and combining weights, they require varying amount of channel state information (CSI) at the relay and the destination. In particular, in order to obtain λ_k at the destination, C–MRC relies on sending γ_{1k} from relay R_k to the destination. In contrast, γ_{2k} and $\bar{\gamma}_{2k}$ have to be feedback from the destination to the kth relay in order to calculate α_k for LAR–α_{inst} and LAR–α, respectively. Since average SNR values tend to vary with considerably slower rates compared to instantaneous SNR values, the

overhead associated the required signaling for LAR–α is considerably lower compared to those of C–MRC and LAR–α_{inst} and this scheme has a higher robustness against outdated CSI. As will be shown in Sections III and IV, this advantage comes at the cost of a diversity loss for LAR–α. special case of C–MRC with $\lambda_1 = 1$.

III. ERROR RATE ANALYSIS

In this section, we provide a unified performance analysis of the C–MRC, LAR–α_{inst}, and LAR–α DF schemes for high SNRs, i.e., for $\bar{\gamma}_0, \bar{\gamma}_{1k}, \bar{\gamma}_{2k} \to \infty$, $1 \leq k \leq K$. In particular, we develop an asymptotic expression for the (average) pairwise error probability (PEP) in Subsection III-A and relate this PEP to the asymptotic (average) SER and BER in Subsection III-B. Furthermore, we employ the developed asymptotic results to analyze the diversity gain achieved by the considered DF schemes in Subsection III-C.

A. Asymptotic PEP

Assuming that $x \in \mathcal{X}$ was transmitted by the source and $\tilde{x} \in \mathcal{X}$, $\tilde{x} \neq x$ was detected at the destination, the PEP for the considered CD system can be expressed as $P(x \to \tilde{x}) = \Pr\{m_c(x) > m_c(\tilde{x})\}$. We use the nearest neighbor approximation for the decoded symbol $\hat{x}_k$ at the relay, i.e., we assume that $\hat{x}_k \in \{x\} \cup \mathcal{N}(x)$, where the set $\mathcal{N}(x)$ contains all nearest neighbors of x in $\mathcal{X}$. This assumption is well justified for $\bar{\gamma}_{1k} \to \infty$ and its accuracy will be confirm by simulation results in Section IV. Based on this assumption the PEP can be written as

$$P(x \to \tilde{x}) = \sum_{i=0}^{|\mathcal{A}|} \left(\Pr\left\{ m_c(x) > m_c(\tilde{x}) \big| \boldsymbol{\nu}_i \right\} \prod_{k=1}^{K} \psi_k(\gamma_{1k}, \nu_{ik}) \right). \tag{6}$$

In (6), $\mathcal{A}$ is the set of all possible values for the decoded signal vector $[\hat{x}_1, \ldots, \hat{x}_K]^T$, i.e., $\mathcal{A} \triangleq \{\boldsymbol{\nu}_i | \boldsymbol{\nu}_i \triangleq [\hat{x}_1, \ldots, \hat{x}_K]^T, \hat{x}_k \in \{x\} \cup \mathcal{N}(x), 1 \leq k \leq K\}$, where i is used to index the elements of $\mathcal{A}$. Furthermore, ν_{ik} denotes the kth element in vector $\boldsymbol{\nu}_i$ and we have defined $\psi_k(\gamma_{1k}, \nu_{ik}) \triangleq 1 - \beta Q\big(\sqrt{2\zeta\,\gamma_{1k}}\big)$ for $\nu_{ik} = x$ and $\psi_k(\gamma_{1k}, \nu_{ik}) \triangleq \frac{\beta}{\mathcal{N}(x)} Q\big(\sqrt{2\zeta\,\gamma_{1k}}\big)$ for $\nu_{ik} \neq x$, where β and ζ are two modulation dependent constants (e.g. $\beta = \zeta = 1$ for BPSK). Using (5) in (6) yields

$$P(x \to \tilde{x}) = \sum_{i=0}^{|\mathcal{A}|} \left(\Pr\{\Delta_0(x, \tilde{x}) + \lambda_k \sum_{k=1}^{K} \Delta_k(x, \tilde{x}, \nu_{ik}) < 0\} \prod_{k=1}^{K} \psi_k(\gamma_{1k}, \nu_{ik}) \right), \tag{7}$$

with $\Delta_0(x, \tilde{x}) \triangleq |\sqrt{\gamma_0}(x - \tilde{x}) + \bar{n}_0|^2 - |\bar{n}_0|^2$ and

$$\Delta_k(x, \tilde{x}, \hat{x}) \triangleq |\sqrt{\gamma_{2k}\alpha_k}(\tilde{x} - \hat{x}_k) + \bar{n}_{2k}|^2 - |\sqrt{\gamma_{2k}\alpha_k}(x - \hat{x}_k) + \bar{n}_{2k}|^2, \qquad 1 \leq k \leq K, \tag{8}$$

where $\bar{n}_0 \triangleq n_0/\sigma_{n_0}$ and $\bar{n}_{2k} \triangleq n_{2k}/\sigma_{n_{2k}}$, $1 \leq k \leq K$. We now exploit that for any RV Δ we have $\mathrm{Pr}\{\Delta < 0\} = \frac{1}{2\pi j}\int_{c-j\infty}^{c+j\infty} \Phi_\Delta(s)\frac{\mathrm{d}s}{s}$ with moment generating function (MGF) $\Phi_\Delta(s) \triangleq \mathcal{E}_\Delta\{e^{-\Delta s}\}$ where c is a small positive constant that lies in the region of convergence of the integrand [8]. This leads to

$$P(x \to \tilde{x}) = \frac{1}{2\pi j} \sum_{i=0}^{|\mathcal{A}|} \int_{c-j\infty}^{c+j\infty} \Phi_0(s) \prod_{k=1}^{K} \Phi_k(s, \nu_{ik}) \frac{\mathrm{d}s}{s}, \tag{9}$$

with

$$\Phi_k(s, \nu_{ik}) \triangleq \begin{cases} \Phi_k^c(s) - \beta\Phi_k^e(s, x), & \nu_{ik} = x \\ \frac{\beta}{\mathcal{N}(x)}\Phi_k^e(s, \nu_{ik}), & \nu_{ik} \neq x \end{cases} \tag{10}$$

where we have defined the MGFs $\Phi_0(s) \triangleq \mathcal{E}_{\gamma_0, \bar{n}_0}\{e^{-s\Delta_0(x,\tilde{x})}\}$, $\Phi_k^c(s) \triangleq \mathcal{E}_{\gamma_{1k}, \gamma_{2k}, \bar{n}_{2k}}\{e^{-s\lambda_k\Delta_k(x,\tilde{x},x)}\}$, and $\Phi_k^e(s, \hat{x}_k) \triangleq \mathcal{E}_{\gamma_{1k}, \gamma_{2k}, \bar{n}_{2k}}\{Q(\sqrt{\zeta\,\gamma_{1k}})\,e^{-s\lambda_k\Delta_k(x,\tilde{x},\hat{x}_k)}\}$. In [6], an asymptotic expression for $\Phi_0(s)$ for $\bar{\gamma}_0 \to \infty$ has been obtained as

$$\Phi_0(s) \overset{\circ}{=} \frac{1}{d_0^2 s(1-s)\bar{\gamma}_0}, \tag{11}$$

where $d_0 \triangleq |\tilde{x} - x|$. Furthermore, asymptotic expressions for $\Phi_k^e(s, \hat{x}_k)$ and $\Phi_k^c(s)$ for $\bar{\gamma}_{1k}, \bar{\gamma}_{2k} \to \infty$ are provided in Table II for C–MRC, LAR–α_{inst}, and LAR–α (The corresponding proofs are provided in the Appendix). With these expressions at hand, the asymptotic PEP can be obtained from (9) and (10) for the considered DF schemes, cf. Section III-B.

B. Asymptotic SER and BER

To obtain an asymptotic expression for the SER we use a truncated union–bound over the asymptotic PEPs $P(x \to \tilde{x})$, where we include only nearest neighbor error events. In particular, a highly accurate approximation for the asymptotic SER is given by

$$P_s \overset{\circ}{=} \frac{\beta}{M} \sum_{x \in \mathcal{X}} \sum_{\tilde{x} \in \mathcal{N}(x)} P(x \to \tilde{x}), \tag{12}$$

To derive a general expression for the SER we first note that according to (10) and Table II, $\Phi_k(s, \nu_{ik})$ can be written as

$$\Phi_k(s, \nu_{ik}) = \frac{\Phi_k^1(s, \nu_{ik})}{\bar{\gamma}_{1k}} + \frac{\Phi_k^2(s, \nu_{ik})}{\bar{\gamma}_{2k}} + \frac{\Phi_k^l(s, \nu_{ik})}{\bar{\gamma}_{lk}}, \tag{13}$$

where $\bar{\gamma}_{lk} \triangleq \frac{\log \bar{\gamma}_{1k}}{\bar{\gamma}_{1k}}$, and $\Phi_k^j(s, \nu_{ik})$, $j \in \{1, 2, l\}$, $1 \leq k \leq K$, can be easily obtained based on (10) and Table II for the considered DF schemes. By combining (9), (11), (12), and (13) we obtain the asymptotic SER as

$$P_s \overset{\circ}{=} \sum_{j_k \in \{1,2,l\},\, 1 \leq k \leq K} C_{j_1 \cdots j_K} \bar{\gamma}_0^{-1} \bar{\gamma}_{j_1 1}^{-1} \cdots \bar{\gamma}_{j_K K}^{-1}, \tag{14}$$

where the coefficients $C_{j_1 \cdots j_K}$, $j_k \in \{1, 2, l\}$, $1 \le k \le K$, are given by

$$C_{j_1 \cdots j_K} \triangleq \frac{\beta}{2\pi j M} \int_{c-j\infty}^{c+j\infty} \bar{\Phi}_0(s) \left(\sum_{x \in \mathcal{X}} \sum_{\tilde{x} \in \mathcal{N}(x)} \sum_{i=0}^{|\mathcal{A}|} \prod_{k=1}^{K} \Phi_k^{j_k}(s, \nu_{ik}) \right) \frac{\mathrm{d}s}{s}, \tag{15}$$

with $\bar{\Phi}_0(s) \triangleq \frac{1}{d_0^2 s(1-s)}$. Furthermore, for Gray labeling the asymptotic BER can be tightly approximated based on the asymptotic SER as

$$P_b \doteq \frac{P_s}{\log_2(M)}. \tag{16}$$

The coefficients $C_{j_1 \cdots j_K}$ in (15) involve a single complex integration which, in general, cannot be obtained in closed–form, and therefore should be obtained numerically, e.g., using the Gauss–Quadrature method [8]. However, for a given DF scheme, signal constellation, and number of relays K, these coefficients have to be calculated only once, and thus the computational complexity associated with the numerical evaluation of the involved complex integrals is not a concern.

In the following examples we demonstrate how (14)–(16) can be employed to obtain an expression for the asymptotic error rate of the C–MRC, LAR–α_{inst}, and LAR–α, respectively, for different number of relays and different modulation formats.

Example 1) In the first example, we consider a CD system employing C–MRC and BPSK modulation. For $K = 2$ relays based on (15) we obtain $C_{11} = 0.4853$, $C_{12} = C_{21} = 0.3435$, and $C_{22} = 0.1562$, while the remaining coefficients are zero. Therefore, using (14)–(16) the asymptotic BER can be expressed as $P_b \doteq \frac{1}{\bar{\gamma}_0} \left(\frac{C_{11}}{\bar{\gamma}_{11}\bar{\gamma}_{12}} + \frac{C_{12}}{\bar{\gamma}_{11}\bar{\gamma}_{22}} + \frac{C_{21}}{\bar{\gamma}_{21}\bar{\gamma}_{12}} + \frac{C_{22}}{\bar{\gamma}_{21}\bar{\gamma}_{22}} \right)$. Similarly, for $K = 1$ relay the asymptotic BER can be expressed as $P_b \doteq \frac{1}{\bar{\gamma}_0} \left(\frac{C_1}{\bar{\gamma}_{11}} + \frac{C_2}{\bar{\gamma}_{21}} \right)$ with $C_1 = 0.2952$ and $C_2 = 0.1875$, which is in agreement with [6, Eq. (25)]. In contrast to AF relaying [2], the asymptotic BER expression for C–MRC is not symmetric with respect to the source–relay and relay–destination links as we have $C_1 \ne C_2$ and $C_{11} \ne C_{22}$ for $K = 1$ and $K = 2$, respectively. For example, for AF and BPSK from [2] we obtain $P_b \doteq \frac{C_0}{\bar{\gamma}_0} \prod_{k=1}^{K} \left(\frac{1}{\bar{\gamma}_{1k}} + \frac{1}{\bar{\gamma}_{2k}} \right)$ with $C_0 = 0.1875$ and $C_0 = 0.1562$ for $K = 1$ and $K = 2$, respectively. As a result of the aforementioned asymmetry of C–MRC, while the channel quality setting $\bar{\gamma}_{2k} = \bar{\gamma}_0 = \bar{\gamma}$, $\bar{\gamma}_{1k} \to \infty$, $1 \le k \le K$, leads to the same asymptotic BER for AF and C–MRC, AF outperforms C–MRC for $\bar{\gamma}_{1k} = \bar{\gamma}_0 = \bar{\gamma}$, $\bar{\gamma}_{2k} \to \infty$, $1 \le k \le K$. This is due to the fact that some information about the transmit signal may be lost when performing hard–decision decoding at the relays (cf. Eq. (3)) which can not be recovered at the destination even if the relay–destination links are ideal.

Example 2) Here, we consider a CD system with LAR–α_{inst} and BPSK modulation. Based on (14)–(16), for $K = 1$ and $K = 2$ we obtain $P_b \doteq \frac{1}{\bar{\gamma}_0} \left(\frac{C_1}{\bar{\gamma}_{11}} + \frac{C_2}{\bar{\gamma}_{21}} \right)$ with $C_1 = 0.4099$ and $C_2 = 0.1875$, and $P_b \doteq \frac{1}{\bar{\gamma}_0} \left(\frac{C_{11}}{\bar{\gamma}_{11}\bar{\gamma}_{12}} + \frac{C_{12}}{\bar{\gamma}_{11}\bar{\gamma}_{22}} + \frac{C_{21}}{\bar{\gamma}_{21}\bar{\gamma}_{12}} + \frac{C_{22}}{\bar{\gamma}_{21}\bar{\gamma}_{22}} \right)$ with $C_{11} = 0.8249$, $C_{12} = C_{21} = 0.4746$, and $C_{22} = 0.1562$, respectively. We note that a similar asymmetry with respect to the source–relay and relay–destination links as in Example 1 is also observed in this case.

Example 3) In the final example, we consider a CD system using LAR–α, $K = 1$ relay, and 8–PSK modulation. Using (14), (15), and $\bar{\gamma}_{l1} = \frac{\log \bar{\gamma}_{11}}{\bar{\gamma}_{11}}$ the asymptotic SER can be expressed as $P_s \doteq \frac{1}{\bar{\gamma}_0} \left(\frac{C_1}{\bar{\gamma}_{11}} + \frac{C_2}{\bar{\gamma}_{21}} + \frac{C_l \log \bar{\gamma}_{11}}{\bar{\gamma}_{11}} \right)$ with $C_1 = -(10.6 + 8.74\, E_1(\bar{\gamma}_{21}/\bar{\gamma}_{11}))$, $C_2 = 8.74\, e^{-\bar{\gamma}_{21}/\bar{\gamma}_{11}}$, $C_l = 8.74$. In this case, C_l is non–zero, and therefore, the asymptotic error rate expression involves a logarithmic term which was not present in the case of C–MRC and LAR–α_{inst}. As will be discussed in the next subsection, this term leads to a diversity loss and therefore a considerable performance degradation for LAR–α at high SNRs.

C. Diversity Gain

The diversity gain is defined as the negative asymptotic slope of error rate curves as a function of the SNR on a double–logarithmic scale and plays a crucial role in the performance of CD system. Therefore, in this subsection we analyze the diversity gain achieved by C–MRC, LAR–α_{inst}, and LAR–α using the asymptotic error rate results obtained in the previous subsection. To formally define the diversity gain we assume without loss of generality that $\bar{\gamma}_0 = \zeta_0 \bar{\gamma}$, $\bar{\gamma}_{1k} = \zeta_{1k} \bar{\gamma}$, and $\bar{\gamma}_{2k} = \zeta_{2k} \bar{\gamma}$, $1 \leq k \leq K$, where ζ_0, ζ_{1k}, and ζ_{2k} are finite (positive) constants, which are independent of $\bar{\gamma}$. The diversity gain associated with the asymptotic SER is then defined as $G_d \triangleq -\lim_{\bar{\gamma} \to \infty} \log(P_s) / \log(\bar{\gamma})$.

For C–MRC and LAR–α_{inst} from (10), Table II, and (13) we have $\Phi_k^l(s, \nu_{ik}) = 0$, and therefore based on (15) we conclude that $C_{j_1 \cdots j_K} = 0$ for $j_k = l$, $1 \leq k \leq K$. As a result, according to (14) we have $P_s \doteq \tilde{\zeta}_1 \bar{\gamma}^{-(K+1)}$, where $\tilde{\zeta}_1$ is a (positive) constant. Therefore the diversity gain is given by $G_d = K + 1$, i.e., a full diversity gain equal to the number of paths between the source and the destination is achieved. However, for LAR–α $\Phi_k^l(s, \nu_{ik})$ and therefore $C_{j_1 \cdots j_K}$ are, in general, non–zero for $j_k = l$, $1 \leq k \leq K$. Consequently, from (14) we obtain $P_s \doteq \tilde{\zeta}_2 \log \bar{\gamma} \, \bar{\gamma}^{-(K+1)}$, where $\tilde{\zeta}_2$ is a (positive) constant. Therefore, the diversity gain achieved by LAR–α is smaller than $K + 1$ but greater than K, i.e., in general, LAR–α is unable to achieve full diversity. As will be shown in Section IV, this diversity loss adversely affects the performance of LAR–α especially at high SNRs.

IV. NUMERICAL AND SIMULATION RESULTS

In this section, we verify the analytical results derived in Sections III with computer simulations. Furthermore, we employ these results to study the performance of C–MRC, LAR–α_{inst}, and LAR–α and to compare the performance of these schemes with that of AF relaying [2]. For the figures in this section, the analytical results were obtained using (14)–(16). Furthermore, we have adopted equal variances for all noise samples (i.e., $\sigma^2_{n_0} = \sigma^2_{n_{1k}} = \sigma^2_{n_{2k}} = N_0$, $1 \leq k \leq K$) and shown the BER as a function of the total per–node average SNR $\bar{\gamma}_t$ defined as $\bar{\gamma}_t \triangleq (1 + \sum_{k=1}^{K} \mathcal{E}\{\alpha_k\})\bar{\gamma}/(K + 1)$ with $\bar{\gamma} \triangleq \frac{p_s}{N_0}$.

In Fig. 2, we show the BERs of CD systems employing C–MRC, LAR–α_{inst}, LAR–α, and AF schemes for $K = 1, 2$ relays. For the considered system we have assumed BPSK modulation and $\bar{\gamma}_{1k} = \bar{\gamma}_{2k} = \bar{\gamma}_0 = \bar{\gamma}$, $1 \leq k \leq K$, i.e., all links have the same quality. As seen from the figure, for high enough SNRs the analytical and simulation results are in excellent agreement confirming that the analytical results provide a suitable means for comparing the performance of the considered schemes. Furthermore, in accordance with Section III-B, a diversity gain of $G_d = K + 1$ is achieved by both C–MRC and LAR–α_{inst}. However, for LAR–α_{inst} the achieved diversity gain is smaller than $K + 1$ (but greater than K) resulting in a substantial performance loss at high SNRs, which increases with the number of relays.

Fig. 3 shows the BER of CD systems employing C–MRC, LAR–α_{inst}, LAR–α, and AF schemes for 8–PSK modulation and $K = 1, 3$ relays. Here, we have assumed $\bar{\gamma}_{1k} = \bar{\gamma}_0 = \bar{\gamma}$ and $\bar{\gamma}_{2k} = \bar{\gamma} + 30\text{dB}$, $1 \leq k \leq K$, and therefore the relay–destination links are much stronger compared to the source–relay links. In contrast to Fig. 3, we observe that LAR–α_{inst} and LAR–α perform considerably better relative to C–MRC. This due to the fact that for the considered channel quality setting LAR–α_{inst} and LAR–α utilize the available transmit power at the relays more efficiently, and consequently for a given $\bar{\gamma}$ achieve a much lower $\bar{\gamma}_t$ compared to C–MRC. However, due to the diversity loss by LAR–α, this performance improvement over C–MRC is significantly reduced or lost for LAR–α at high SNRs.

V. CONCLUSIONS

In this paper, we have provided a performance analysis of C–MRC, LAR–α_{inst}, and LAR–α DF schemes for multi–branch CD systems for high SNRs and Rayleigh fading. The developed analytical results a) are valid for arbitrary modulation formats and arbitrary channel qualities b) facilitate a performance comparison with other relaying schemes c) reveal that for CD systems with K relays

C–MRC and LAR–α_{inst} achieve the full diversity gain of $G_d = K + 1$, but the diversiy gain achieved by LAR–α is between K and $K + 1$, i.e., LAR–α is, in general, unable to achieve full diversity.

APPENDIX

In this appendix, we analyze the asymptotic behavior of $\Phi_k^e(s, \hat{x}_k)$ for $\bar{\gamma}_{1k}, \bar{\gamma}_{2k} \to \infty$, $1 \leq k \leq K$, for C–MRC, LAR–α_{inst}, and LAR–α, respectively. The asymptotic behavior of $\Phi_k^c(s)$ can be obtained in a similar manner for the considered DF schemes. The resulting asymptotic expressions for $\Phi_k^e(s, \hat{x}_k)$ and $\Phi_k^c(s)$ are provided in Table II. For simplicity, we drop the subscript k in the following.

Using the alternative representation for the Q–function $Q(x) = \frac{1}{\pi} \int_0^{\pi/2} e^{-x^2/\sin^2 \theta} d\theta$ we can write $\Phi^e(s, \hat{x})$ as

$$\Phi^e(s, \hat{x}) = \frac{1}{\pi} \int_0^{\pi/2} \Phi(s, \theta) \, d\theta, \tag{17}$$

where $\Phi(s, \theta) \triangleq \mathcal{E}_{\gamma_1, \gamma_2, \bar{n}_2} \{ e^{-\frac{\zeta \gamma_1}{\sin^2 \theta}} e^{-s\lambda \Delta(x, \tilde{x}, \hat{x})} \}$. Using (8) and the relation $\mathcal{E}_{\bar{n}_2} \{ e^{-s \Re\{\bar{n}_2^*\}} \} = e^{s^2}$, $\Phi(s, \theta)$ can be expressed as

$$\Phi(s, \theta) = \frac{1}{\bar{\gamma}_1 \bar{\gamma}_2} \int_0^\infty \int_0^\infty e^{-s\lambda \alpha \gamma_2 \, d(\hat{x}) + s^2 \lambda^2 \alpha \gamma_2 \, d_0^2 - \frac{\zeta \gamma_1}{\sin^2 \theta}} e^{-\gamma_1/\bar{\gamma}_1} e^{-\gamma_2/\bar{\gamma}_2} d\gamma_1 \, d\gamma_2, \tag{18}$$

where $d(\hat{x}) \triangleq |\tilde{x} - \hat{x}|^2 - |x - \hat{x}|^2$. In the following, we employ (17) and (18) to obtain the asymptotic behavior of $\Phi^e(s, \hat{x})$ for C–MRC, LAR–α_{inst}, and LAR–α, respectively.

C–MRC: The asymptotic behavior of $\Phi(s, \theta)$ for $\bar{\gamma}_1, \bar{\gamma}_2 \to \infty$ has been obtained in [6] as $\Phi(s, \theta) \doteq \frac{1}{(d(\hat{x})s + \frac{\zeta}{\sin^2 \theta}) \bar{\gamma}_1}$, where we have adjusted the notation of [6] to the problem at hand. Applying this result in (17) leads to the asymptotic expression given in Table II for $\Phi^e(s, \hat{x})$ and C–MRC.

LAR–α_{inst}: For LAR–α_{inst} based on (18) and Table I we obtain

$$\Phi(s, \theta) = \frac{1}{\bar{\gamma}_1 \bar{\gamma}_2} \int_0^\infty \int_0^\infty e^{-s \min\{\gamma_1, \gamma_2\} \, d(\hat{x}) - \frac{\zeta \gamma_1}{\sin^2 \theta}} e^{s^2 \min\{\gamma_1, \gamma_2\} \, d_0^2} e^{-\gamma_1/\bar{\gamma}_1} e^{-\gamma_2/\bar{\gamma}_2} \, d\gamma_1 \, d\gamma_2. \tag{19}$$

Splitting the inner integration interval in (19) into two intervals $[0, \gamma_1)$ and $[\gamma_1, \infty)$ results in $\Phi(s, \theta) = \Phi_1(s, \theta) + \Phi_2(s, \theta)$ where

$$\Phi_1(s, \theta) \triangleq \frac{1}{\bar{\gamma}_1 \bar{\gamma}_2} \int_0^\infty d\gamma_1 \, e^{-\gamma_1 (\frac{\zeta}{\sin^2 \theta} + 1/\bar{\gamma}_1)} \int_0^{\gamma_1} d\gamma_2 e^{-\gamma_2 (s \, d(\hat{x}) - s^2 \, d_0^2 + 1/\bar{\gamma}_2)}, \tag{20}$$

and

$$\Phi_2(s, \theta) \triangleq \frac{1}{\bar{\gamma}_1 \bar{\gamma}_2} \int_0^\infty d\gamma_1 \, e^{-\gamma_1 (s \, d(\hat{x}) + \frac{\zeta}{\sin^2 \theta} - s^2 \, d_0^2 + 1/\bar{\gamma}_1)} \int_{\gamma_1}^\infty d\gamma_2 \, e^{-\gamma_2/\bar{\gamma}_2}. \tag{21}$$

For $\Phi_1(s, \theta)$ based on (20) we obtain

$$\Phi_1(s, \theta) = \frac{1}{\bar{\gamma}_1 \bar{\gamma}_2 \left(s \, d(\hat{x}) - s^2 \, d_0^2 + 1/\bar{\gamma}_2 + \frac{\zeta}{\sin^2 \theta} + 1/\bar{\gamma}_1 \right) \left(\frac{\zeta}{\sin^2 \theta} + 1/\bar{\gamma}_1 \right)} \doteq o\left(\bar{\gamma}_1^{-1} \bar{\gamma}_2^{-1}\right). \tag{22}$$

For $\Phi_2(s,\theta)$ from (21) we get

$$\Phi_2(s,\theta) = \frac{1}{\bar{\gamma}_1} \int_0^\infty \mathrm{d}\gamma_1 \, \mathrm{e}^{-\gamma_1\left(s\,d(\hat{x}) + \frac{\zeta}{\sin^2\theta} - s^2\,d_0^2 + 1/\bar{\gamma}_1 + 1/\bar{\gamma}_2\right)} \doteq \frac{1}{\bar{\gamma}_1\left(s\,d(\hat{x}) + \frac{\zeta}{\sin^2\theta} - s^2\,d_0^2\right)}. \qquad (23)$$

The asymptotic behavior of $\Phi^e(s,\hat{x})$ can be obtained as given in Table II by combining (22), (23), and (17).

LAR–α: For LAR–α from (18) and Table I we have

$$\Phi(s,\theta) = \frac{1}{\bar{\gamma}_1\bar{\gamma}_2} \int_0^\infty \int_0^\infty \mathrm{e}^{-s\min\{\gamma_1,\bar{\gamma}_2\}/\bar{\gamma}_2\,\gamma_2 d(\hat{x}) - \frac{\zeta\,\gamma_1}{\sin^2\theta} + s^2\min\{\gamma_1,\bar{\gamma}_2\}/\bar{\gamma}_2\,\gamma_2\,d_0^2} \, \mathrm{e}^{-\gamma_1/\bar{\gamma}_1} \, \mathrm{e}^{-\gamma_2/\bar{\gamma}_2} \, \mathrm{d}\gamma_1 \, \mathrm{d}\gamma_2. \quad (24)$$

Splitting the inner integration interval in (19) into two intervals $[0,\bar{\gamma}_2)$, $[\bar{\gamma}_2,\infty)$ results in $\Phi(s,\theta) = \Phi_1(s,\theta) + \Phi_2(s,\theta)$, where

$$\Phi_1(s,\theta) \triangleq \frac{1}{\bar{\gamma}_1\bar{\gamma}_2} \int_0^\infty \mathrm{d}\gamma_2 \, \mathrm{e}^{-\gamma_2/\bar{\gamma}_2} \int_0^{\bar{\gamma}_2} \mathrm{d}\gamma_1 \mathrm{e}^{-\gamma_1\left(s\gamma_2/\bar{\gamma}_2 d(\hat{x}) + \frac{\zeta}{\sin^2\theta} - s^2\gamma_2/\bar{\gamma}_2\,d_0^2 + 1/\bar{\gamma}_1\right)}, \qquad (25)$$

and

$$\Phi_2(s,\theta) = \frac{1}{\bar{\gamma}_1\bar{\gamma}_2} \int_0^\infty \mathrm{d}\gamma_2 \, \mathrm{e}^{-\gamma_2\left(sd(\hat{x}) + s^2\,\gamma_2\,d_0^2 + 1/\bar{\gamma}_2\right)} \int_{\bar{\gamma}_2}^\infty \mathrm{d}\gamma_1 \mathrm{e}^{-\frac{\zeta\,\gamma_1}{\sin^2\theta}} \, \mathrm{e}^{-\gamma_1/\bar{\gamma}_1}. \qquad (26)$$

Using (25), $\Phi_1(s,\theta)$ can be written as

$$\Phi_1(s,\theta) \doteq \frac{1}{\bar{\gamma}_1} \int_0^\infty \frac{\mathrm{e}^{-\gamma_2'} \, \mathrm{d}\gamma_2'}{s\gamma_2' d(\hat{x}) + \frac{\zeta}{\sin^2\theta} - s^2\,\gamma_2'\,d_0^2}. \qquad (27)$$

For $\Phi_2(s,\theta)$ from (26) we obtain

$$\Phi_2(s,\theta) = \frac{\mathrm{e}^{-\left(\frac{\zeta}{\sin^2\theta} + 1/\bar{\gamma}_1\right)\bar{\gamma}_2}}{\left(\frac{\zeta}{\sin^2\theta} + 1/\bar{\gamma}_1\right)\bar{\gamma}_1\bar{\gamma}_2} \int_0^\infty \mathrm{d}\gamma_2 \, \mathrm{e}^{-\gamma_2\left(sd(\hat{x}) + s^2\,\gamma_2\,d_0^2 + 1/\bar{\gamma}_2\right)} \doteq o\left(\mathrm{e}^{-\frac{\zeta\bar{\gamma}_2}{\sin^2\theta}}\bar{\gamma}_1^{-1}\bar{\gamma}_2^{-1}\right). \qquad (28)$$

By combining (27), (28), and (17) we arrive at the asymptotic expression given in Table II for $\Phi^e(s,\hat{x})$ and LAR–α.

REFERENCES

[1] T. Wang, A. Cano, G.B. Giannakis, and J.N. Laneman. High–Performance Cooperative Demodulation With Decode–and–Forward Relays. *IEEE Trans. Commun.*, 55:1427–1438, July 2007.

[2] A.C. Ribeiro and G.B. Giannakis. Symbol Error Probabilities for General Cooperative Links. *IEEE Wireless Commun.*, 4:1264–1273, May 2005.

[3] A. Sendonaris, E. Erkip, and B. Aazhang. User Cooperation Diversity – Parts I and II. *IEEE Trans. Commun.*, COM-51:1927–1948, November 2003.

[4] J.N. Laneman, D.N.C. Tse, and G.W. Wornell. Cooperative Diversity in Wireless Networks: Efficient Protocols and Outage Behavior. *IEEE Trans. Inform. Theory*, 50:3062–3080,, December 2004.

[5] T. Wang, G.B. Giannakis, and R. Wang;. Smart Regenerative Relays for Link–Adaptive Cooperative Communications. *IEEE Trans. Commun.*, 56:1950–1960, November 2008.

[6] A. Nasri, R. Schober, and M. Uysal. Error Performance of Network-Coded Cooperative Diversity. *Accepted for pulication at the IEEE Global Telecommun. Conf. (Globecom)*, December 2010.

[7] M.O. Hasna and M.S. Alouini. End-to-End Performance of Transmission Systems with Relays Over Rayleigh–Fading Channels. *IEEE Wireless Commun.*, 2:1126–1131, November 2003.

[8] E. Biglieri, G. Caire, G. Taricco, and J. Ventura-Traveset. Computing Error Probabilities over Fading Channels: a Unified Approach. *European Trans. Telecommun.*, 9:15–25, Jan./Feb. 1998.

TABLE I
RELAY GAIN α_k AND COMBINING WEIGHT λ_k FOR C–MRC [1], LAR–α_{inst}, AND LAR–α [5].

Scheme	α_k	λ_k
C–MRC	1	$\frac{\min\{\gamma_{1k},\gamma_{2k}\}}{\gamma_{2k}}$
LAR–α_{inst}	$\frac{\min\{\gamma_{1k},\gamma_{2k}\}}{\gamma_{2k}}$	1
LAR–α	$\frac{\min\{\gamma_{1k},\bar{\gamma}_{2k}\}}{\bar{\gamma}_{2k}}$	1

TABLE II
ASYMPTOTIC BEHAVIOR OF $\Phi_k^e(s,\hat{x}_k)$ AND $\Phi_k^c(s)$ FOR $\bar{\gamma}_{1k}, \bar{\gamma}_{2k} \to \infty$ FOR C–MRC, LAR–α_{inst}, AND LAR–α. HERE, WE HAVE USED $d(\hat{x}_k) = |\tilde{x} - \hat{x}_k|^2 - |x - \hat{x}_k|^2$, $\eta(s,\hat{x}_k) \triangleq (sd(\hat{x}_k) - s^2 d_0^2)/\zeta$, AND $\xi_k \triangleq \bar{\gamma}_{2k}/\bar{\gamma}_{1k}$. FURTHERMORE, $\Gamma(\cdot)$, $\mathrm{erf}(\cdot)$, $\mathrm{erfi}(\cdot)$, $E_1(\cdot)$, $_p\mathcal{F}_q(\{\alpha_1,\cdots,\alpha_p\};\{\beta_1,\cdots,\beta_q\};\cdot)$, AND γ_o DENOTE THE GAMMA FUNCTION, THE ERROR FUNCTION, THE IMAGINARY ERROR FUNCTION, THE EXPONENTIAL INTEGRAL FUNCTION, THE GENERALIZED HYPERGEOMETRIC FUNCTION OF ORDER (p,q), AND THE EULER CONSTANT, RESPECTIVELY.

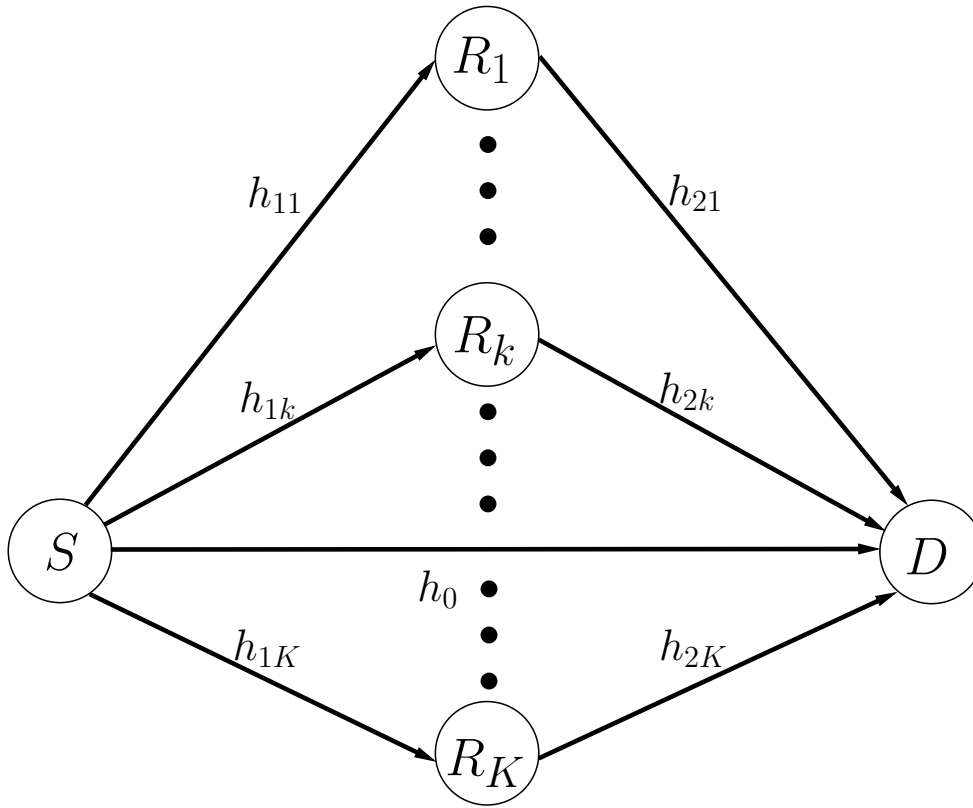| Scheme	Asymptotic $\Phi_k^e(s,\hat{x}_k)$	Asymptotic $\Phi_k^c(s)$
C–MRC	$\frac{1}{2d(\hat{x}_k)s\bar{\gamma}_{1k}}\left(1 - \frac{\zeta}{\sqrt{d(\hat{x}_k)s\,\zeta + \zeta^2}}\right)$	$\frac{1}{\bar{\gamma}_{1k}d_0^2 s} + \frac{1}{\bar{\gamma}_{2k}d_0^2 s(1-s)}$
LAR–α_{inst}	$\frac{1}{2(d(\hat{x}_k)s - s^2 d_0^2)\bar{\gamma}_{1k}}\left(1 - \frac{\zeta}{\sqrt{(d(\hat{x}_k)s - s^2 d_0^2)\,\zeta + \zeta^2}}\right)$	$\frac{1}{s(1-s)d_0^2}\left(\frac{1}{\bar{\gamma}_{1k}} + \frac{1}{\bar{\gamma}_{2k}}\right)$
LAR–α	$-\frac{1}{6\,\zeta(\eta(s,\hat{x}_k))^2\bar{\gamma}_{1k}}\Big[2\,_2\mathcal{F}_2\big(\{1,1\};\{2,5/2\};\frac{1}{\eta(s,\hat{x}_k)}\big)$ $+3\,\eta(s,\hat{x}_k)\Big(\sqrt{\pi\,\eta(s,\hat{x}_k)}\,\mathrm{e}^{1/\eta(s,\hat{x}_k)}\mathrm{erf}(1/\sqrt{\eta(s,\hat{x}_k)})$ $-\pi\,\mathrm{erfi}(1/\sqrt{\eta(s,\hat{x}_k)}) - \log\eta(s,\hat{x}_k) + \gamma_o + \log 4 - 2\Big)\Big]$	$\frac{1}{s(1-s)d_0^2\bar{\gamma}_{1k}}\Big(-E_1(\xi_k) + \log(s(1-s)d_0^2) - \gamma_o\Big)$ $+\frac{\mathrm{e}^{-\xi_k}}{s(1-s)d_0^2\bar{\gamma}_{2k}} + \frac{1}{s(1-s)d_0^2\bar{\gamma}_{lk}}$

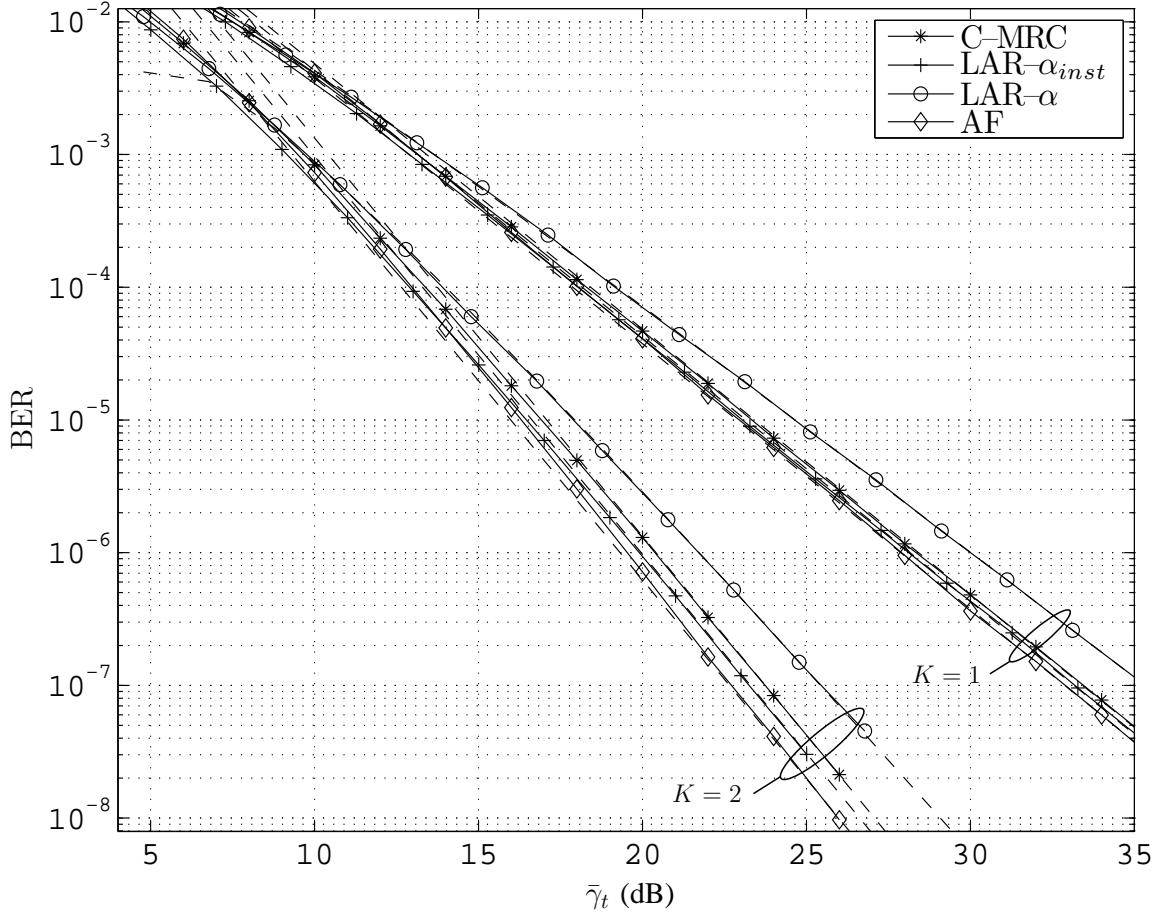Fig. 1.   Block diagram for the considered multi–branch CD system.

Fig. 2. BER vs. $\bar{\gamma}$ for CD systems employing C–MRC, LAR–α_{inst}, LAR–α, and AF schemes for $K = 1, 2$ relays, BPSK modulation, and $\bar{\gamma}_{1k} = \bar{\gamma}_{2k} = \bar{\gamma}_0 = \bar{\gamma}$, $1 \leq k \leq K$. Solid lines with markers: Simulated BER. Dashed line: Asymptotic BER.
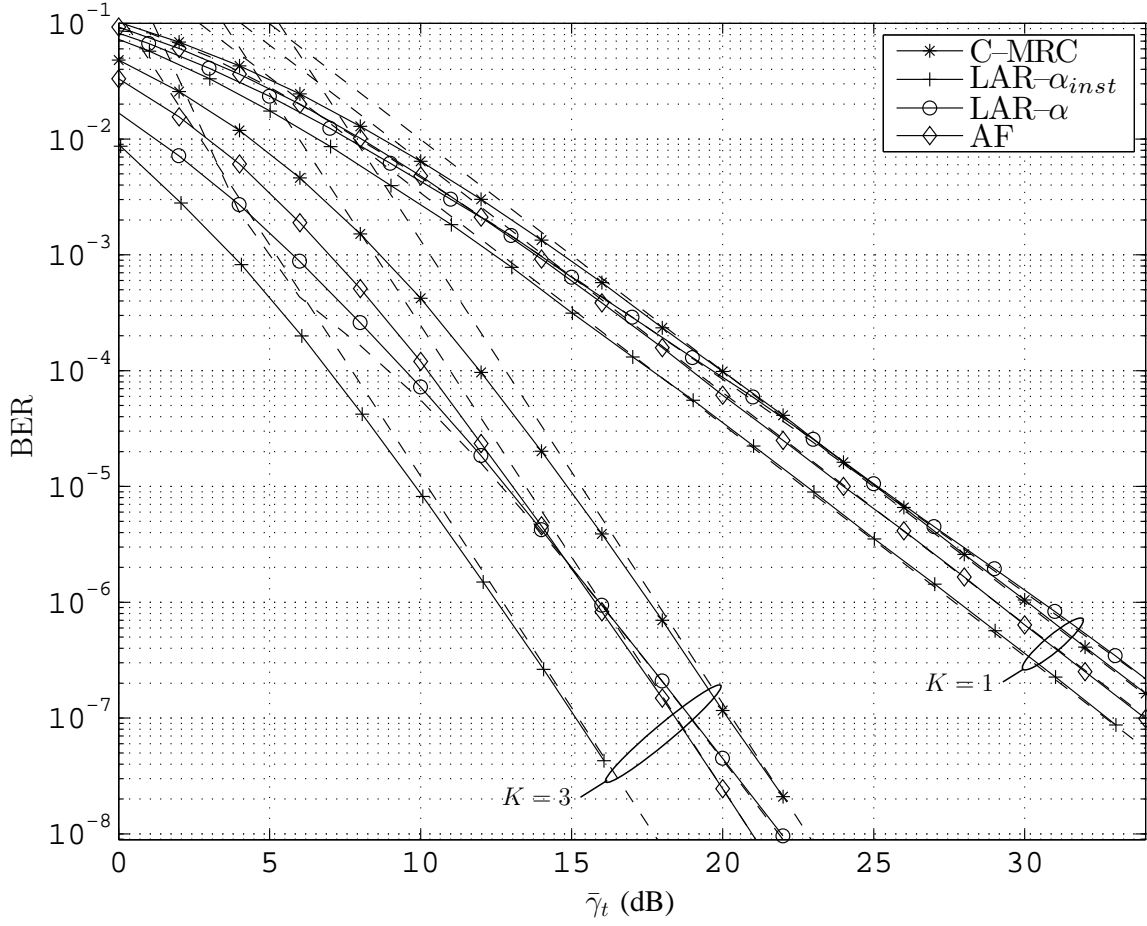
Fig. 3. BER vs. $\bar{\gamma}$ for CD systems employing C–MRC, LAR–α_{inst}, LAR–α, and AF schemes for $K = 1, 3$ relays, 8–PSK modulation, and $\bar{\gamma}_{1k} = \bar{\gamma}_0 = \bar{\gamma}$, $\bar{\gamma}_{2k} = \bar{\gamma} + 30$dB, $1 \leq k \leq K$. Solid lines with markers: Simulated BER. Dashed line: Asymptotic BER.